Momentum Distribution and Condensate Fraction of a Fermion Gas in the BCS-BEC Crossover

G. E. Astrakharchik,[1,2] J. Boronat,[3] J. Casulleras,[3] and S. Giorgini[4,1]

[1]*Dipartimento di Fisica and BEC-INFM, Università di Trento, I-38050 Povo, Italy*

[2]*Institute of Spectroscopy, 142190 Troitsk, Moscow region, Russia*

[3]*Departament de Física i Enginyeria Nuclear, Campus Nord B4-B5, Universitat Politècnica de Catalunya, E-08034 Barcelona, Spain*

[4]*JILA, University of Colorado, Boulder, Colorado 80309-0440, USA*

(Received 20 July 2005; published 1 December 2005)

By using the diffusion Monte Carlo method we calculate the one- and two-body density matrix of an interacting Fermi gas at $T = 0$ in the BCS to Bose-Einstein condensate (BEC) crossover. Results for the momentum distribution of the atoms, as obtained from the Fourier transform of the one-body density matrix, are reported as a function of the interaction strength. Off-diagonal long-range order in the system is investigated through the asymptotic behavior of the two-body density matrix. The condensate fraction of pairs is calculated in the unitary limit and on both sides of the BCS-BEC crossover.

DOI: 10.1103/PhysRevLett.95.230405 PACS numbers: 03.75.Hh, 05.30.Fk, 21.65.+f

The physics of the crossover from Bardeen-Cooper-Schrieffer (BCS) superfluids to molecular Bose-Einstein condensates (BECs) in ultracold Fermi gases near a Feshbach resonance is a very exciting field that has recently attracted a lot of interest, both from the experimental [1,2] and the theoretical side [3]. An important experimental achievement is the observation of a condensate of pairs of fermionic atoms on the side of the Feshbach resonance where no stable molecules would exist in vacuum [4,5]. Although the interpretation of the experiment is not straightforward, as it involves an out-of-equilibrium projection technique of fermionic pairs onto bound molecules [6], it is believed that these results strongly support the existence of a superfluid order parameter in the strongly correlated regime on the BCS side of the resonance [5].

The occurrence of off-diagonal long-range order (ODLRO) in interacting systems of bosons and fermions was investigated by C. N. Yang in terms of the asymptotic behavior of the one- and two-body density matrix [7]. In the case of a two-component Fermi gas with $N_\uparrow$ spin-up and $N_\downarrow$ spin-down particles, the one-body density matrix (OBDM) for spin-up particles, defined as

$$\rho_1(\mathbf{r}_1', \mathbf{r}_1) = \langle \psi_\uparrow^\dagger(\mathbf{r}_1')\psi_\uparrow(\mathbf{r}_1)\rangle, \tag{1}$$

does not possess any eigenvalue of order $N_\uparrow$. This behavior implies for homogeneous systems the asymptotic condition $\rho_1(\mathbf{r}_1', \mathbf{r}_1) \to 0$ as $|\mathbf{r}_1 - \mathbf{r}_1'| \to \infty$. In the above expression $\psi_\uparrow^\dagger(\mathbf{r})$ [$\psi_\uparrow(\mathbf{r})$] denote the creation (annihilation) operator of spin-up particles. The same result holds for spin-down particles. ODLRO may occur instead in the two-body density matrix (TBDM), that is defined as

$$\rho_2(\mathbf{r}_1', \mathbf{r}_2', \mathbf{r}_1, \mathbf{r}_2) = \langle \psi_\uparrow^\dagger(\mathbf{r}_1')\psi_\downarrow^\dagger(\mathbf{r}_2')\psi_\uparrow(\mathbf{r}_1)\psi_\downarrow(\mathbf{r}_2)\rangle. \tag{2}$$

For a homogeneous unpolarized gas with $N_\uparrow = N_\downarrow = (N/2)$, if ρ_2 has an eigenvalue of the order of the total number of particles N, the TBDM can be written as a spectral decomposition separating the largest eigenvalue yielding for $|\mathbf{r}_1 - \mathbf{r}_1'|$, $|\mathbf{r}_2 - \mathbf{r}_2'| \to \infty$ the asymptotic behavior

$$\rho_2(\mathbf{r}_1', \mathbf{r}_2', \mathbf{r}_1, \mathbf{r}_2) \to \alpha N/2 \varphi^*(|\mathbf{r}_1' - \mathbf{r}_2'|)\varphi(|\mathbf{r}_1 - \mathbf{r}_2|). \tag{3}$$

The parameter $\alpha \leq 1$ is interpreted as the condensate fraction of pairs, in a similar way as the condensate fraction of single atoms is derived from the OBDM. The complex function $\varphi(r)$ is normalized to the inverse volume $(1/V)$ and is proportional to the order parameter $\langle \psi_\uparrow(\mathbf{r}_1)\psi_\downarrow(\mathbf{r}_2)\rangle = \sqrt{\alpha N/2}\varphi(|\mathbf{r}_1 - \mathbf{r}_2|)$, whose appearance distinguishes the superfluid state of the Fermi gas. Equation (3) should be contrasted with the behavior of Bose systems with ODLRO, where ρ_1 has an eigenvalue of order N [8], and consequently the largest eigenvalue of ρ_2 is of the order of N^2.

In this Letter we present fixed-node diffusion Monte Carlo (FN DMC) results of ρ_1 and ρ_2 for a homogeneous interacting Fermi gas at $T = 0$ in the BCS-BEC crossover. From the Fourier transform of $\rho_1(r)$, we calculate the momentum distribution of the gas, $n_\mathbf{k} = \int d^3\mathbf{r}\rho_1(r)e^{i\mathbf{k}\cdot\mathbf{r}}$, as a function of the interaction strength. From the asymptotic behavior of ρ_2, we extract the value of the condensate fraction of pairs α. The calculated condensate fraction is compared with analytical expansions holding on the BEC and BCS sides of the Feshbach resonance. The comparison with mean-field results [9] for $n_\mathbf{k}$ and α is also discussed.

We consider a homogeneous two-component unpolarized Fermi gas described by the Hamiltonian

$$H = -\frac{\hbar^2}{2m}\left(\sum_{i=1}^{(N/2)}\nabla_i^2 + \sum_{i'=1}^{(N/2)}\nabla_{i'}^2\right) + \sum_{i,i'}V(r_{ii'}), \tag{4}$$

where m is the mass of the particles and $i, j, \ldots$ $(i', j', \ldots)$ label spin-up (spin-down) particles. The strength of the interaction is assumed to be determined only by the parameter $1/k_F a$, with $k_F = (3\pi^2 n)^{1/3}$ the Fermi wave-

vector fixed by the atomic density $n = N/V$, and a the s-wave scattering length describing the low-energy collisions between the two fermionic species. The interatomic interactions in Eq. (4) are only between atoms with different spin and are modeled by a short-range potential that determines the value of a. In the present study, we use an attractive square-well potential, $V(r) = -V_0$ for $r < R_0$ and $V(r) = 0$ otherwise, with $nR_0^3 = 10^{-6}$. We have verified that in the density range $nR_0^3 = 10^{-7} - 10^{-5}$ the particular form of $V(r)$ is not relevant, and therefore the present results are in this sense universal. The different regimes: BEC ($a > 0$ and $1/k_F a \gg 1$), BCS ($a < 0$ and $1/k_F|a| \gg 1$), and unitary limit ($1/k_F a = 0$), are obtained by varying the potential depth V_0 as in Ref. [10]. Quantum Monte Carlo studies of the Hamiltonian (4) have already been carried out to investigate the $T = 0$ equation of state [10–12] and the pairing gap [11,12].

In a FN DMC simulation, the wave function $f(\mathbf{R}, \tau) = \psi_T(\mathbf{R})\Psi(\mathbf{R}, \tau)$ ($\mathbf{R} = \mathbf{r}_1, \ldots, \mathbf{r}_{N_\uparrow}, \mathbf{r}_{1'}, \ldots, \mathbf{r}_{N_\downarrow}$) is evolved in imaginary time $\tau = it/\hbar$ according to the time-dependent Schrödinger equation, with $\psi_T(\mathbf{R})$ acting as importance sampling function and as nodal constraint. The function $\Psi(\mathbf{R}) \equiv \Psi(\mathbf{R}, \tau \to \infty)$, which is the lowest energy state of the system having the nodes of $\psi_T(\mathbf{R})$, is obtained from the large-time evolution of $f(\mathbf{R}, \tau)$. The trial wave function we consider has the general form [11–13] $\psi_T(\mathbf{R}) = \Psi_J(\mathbf{R})\Psi_{BCS}(\mathbf{R})$, where Ψ_J contains Jastrow correlations between all the particles,

$$\Psi_J(\mathbf{R}) = \prod_{i<j} f_{\uparrow\uparrow}(r_{ij}) \prod_{i'<j'} f_{\downarrow\downarrow}(r_{i'j'}) \prod_{i,i'} f_{\uparrow\downarrow}(r_{ii'}), \qquad (5)$$

and the BCS-type wave function Ψ_{BCS} is the antisymmetrized product of the pair wave functions $\phi(\mathbf{r}_i - \mathbf{r}_{i'})$

$$\Psi_{BCS}(\mathbf{R}) = \mathcal{A}(\phi(\mathbf{r}_1 - \mathbf{r}_{1'})\phi(\mathbf{r}_2 - \mathbf{r}_{2'}) \ldots \phi(\mathbf{r}_{N_\uparrow} - \mathbf{r}_{N_\downarrow})). \qquad (6)$$

The pair orbital $\phi(\mathbf{r})$ is chosen as

$$\phi(\mathbf{r}) = \beta \sum_{k_\alpha \le k_{\max}} e^{i\mathbf{k}_\alpha \cdot \mathbf{r}} + \phi_s(r), \qquad (7)$$

where the sum is performed over the plane wave states $\mathbf{k}_\alpha = 2\pi/L(\ell_{\alpha x}\hat{\mathbf{x}} + \ell_{\alpha y}\hat{\mathbf{y}} + \ell_{\alpha z}\hat{\mathbf{z}})$ up to the largest closed shell $k_{\max} = 2\pi/L(\ell_{x\,\max x}^2 + \ell_{\max y}^2 + \ell_{\max z}^2)^{1/2}$ occupied by $N/2$ particles. Here $L = V^{1/3}$ is the size of the cubic simulation box and ℓ are integer numbers. If $\phi_s(r) = 0$ in Eq. (7), Ψ_{BCS} in Eq. (6) coincides with the exact wave function of a free Fermi gas, i.e., the product of Slater determinants of spin-up and spin-down particles [14]. The spherically symmetric function $\phi_s(r)$ in Eq. (7) accounts for s-wave pairing. If $1/k_F a \ge -0.2$, $\phi_s(\mathbf{r})$ corresponds to the solution of the two-body problem with the potential $V(r)$, as in Ref. [10]. For $1/k_F a < -0.2$ we use instead $\phi_s(r) = \gamma_1\{\exp(-\gamma_2 r) + \exp[-\gamma_2(L - r)]\}$. Here, γ_1, γ_2, and β in Eq. (7) are variational parameters.

The Jastrow wave function Ψ_J, Eq. (5), is determined as follows. For $1/k_F a \ge -0.2$, we use $f_{\uparrow\downarrow}(r) = 1$ and $f_{\uparrow\uparrow}(r) = f_{\downarrow\downarrow}(r)$ given by the two-body solution of a fictitious repulsive step potential with range $\tilde{R}$ and scattering length $\tilde{a}$. The boundary conditions $f(r = L/2) = 1$ and $f'(r = L/2) = 0$ determine the wave function in terms of the variational parameters $\tilde{R}$ and $\tilde{a}$. For $1/k_F a < -0.2$, we use instead $f_{\uparrow\uparrow}(r) = f_{\downarrow\downarrow}(r) = 1$ and the model used in Ref. [10] for the crossed correlation factor, $f_{\uparrow\downarrow}(r)$. It is worth noticing that the function $\psi_T(\mathbf{R})$ defined above reproduces as a special case the trial wave function used in the preceding study [10], but contains more variational parameters. The parameters of the Jastrow function Ψ_J, Eq. (5), are optimized by minimizing the variational expectation value $\langle\psi_T|H|\psi_T\rangle/\langle\psi_T|\psi_T\rangle$. The parameters of the BCS function Ψ_{BCS}, Eq. (6), affect the nodal surface of the trial wave function and they are optimized by minimizing the FN DMC estimate of the energy. For the values of $1/k_F a$ used in the present study, the calculated FN DMC energies are in agreement with the results obtained in Ref. [10], although the optimized variational energy has significantly improved.

A direct estimate of any operator O in DMC is known as mixed estimate, $\langle O\rangle_m = \langle\psi_T|O|\Psi\rangle/\langle\psi_T|\Psi\rangle$, and is exact only for the Hamiltonian and operators commuting with it. If O is a local operator, one can circumvent this problem by introducing pure estimators. That is not the case for ρ_1 and ρ_2 which are the objectives of the present work. In order to reduce, and even eliminate in practice, a possible bias in the calculation we have used the extrapolated estimator $\langle\Psi|O|\Psi\rangle/\langle\Psi|\Psi\rangle \simeq 2\langle O\rangle_m - \langle O\rangle_v$, with $\langle O\rangle_v = \langle\psi_T|O|\psi_T\rangle/\langle\psi_T|\psi_T\rangle$ [13].

We consider a system with $N = 66$ particles and periodic boundary conditions. In Fig. 1 we show results of the OBDM $\rho_1(r)$, Eq. (1), for different values of the interaction strength $1/k_F a$. In the deep molecular regime, $1/k_F a \gg 1$,

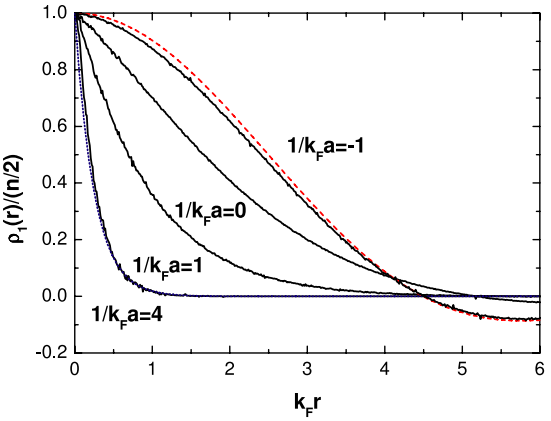

FIG. 1 (color online). OBDM for different values of the interaction strentgth $1/k_F a$ (solid lines). The dotted line (blue online) corresponds to $e^{-r/a}$ for $1/k_F a = 4$ and the dashed line (red online) is the OBDM of a non interacting gas.

the OBDM is determined by the molecular wave function $\phi_{\rm bs}(r)$: $\rho_1(r) \simeq (n/2)\int d^3\mathbf{r}'\phi^*_{\rm bs}(|\mathbf{r}+\mathbf{r}'|)\phi_{\rm bs}(r')$. For a zero-range potential the molecular wave function is given by $\phi_{\rm bs}(r) \propto e^{-r/a}/r$ and one finds $\rho_1(r) \simeq ne^{-r/a}/2$. This behavior is shown in Fig. 1 for $1/k_Fa = 4$. If one moves closer to the resonance, the OBDM decays slowly and oscillations start to appear. Finally, on the BCS side of the resonance, the OBDM becomes more and more similar to the ideal gas result $\rho_1(r) = 3n[\sin(k_Fr)/(k_Fr) - \cos(k_Fr)]/[2(k_Fr)^2]$. The momentum distribution $n_{\mathbf{k}}$, obtained from the Fourier transform of $\rho_1(r)$, is shown in Fig. 2. In the inset of Fig. 2 we compare $n_{\mathbf{k}}$, calculated using FN DMC for $1/k_Fa = 4$, with the momentum distribution of the atoms in the molecular state $n_{\mathbf{k}} = 4(k_Fa)^3/[3\pi(1+k^2a^2)^2]$ [15]. To reduce finite-size effects in the calculation of the Fourier transform for $1/k_Fa = 0$ and -1, we have used the following model for the k dependence of $n_{\mathbf{k}}$

$$n_{\mathbf{k}} = A\left(1 - \frac{(k/k_F)^2 - \mu}{\sqrt{[(k/k_F)^2 - \mu]^2 + \Delta^2}}\right). \quad (8)$$

The values of μ, Δ, and A are free parameters determined by the best fit of the inverse Fourier transform of Eq. (8) to the calculated $\rho_1(r)$, with the constraint $(1/V)\sum_k n_{\mathbf{k}} = (n/2)$. For $A = 1/2$, the above expression reproduces the standard $n_{\mathbf{k}}$ of BCS theory with μ and Δ, respectively, the chemical potential and gap in units of the Fermi energy $\epsilon_F = \hbar^2k_F^2/2m$. For $1/k_Fa = 0$ and -1 the Fourier transform of the BCS model, Eq. (8), reproduces quite well the calculated $\rho_1(r)$ with a χ^2/ν of the order of 1. In Fig. 2 we also show the results of $n_{\mathbf{k}}$ obtained using the BCS mean-field theory [9], where the values of chemical potential and gap are calculated self-consistently through the gap and number equations [15]. The results of Fig. 2 show that the mean-field theory overestimates the broadening of $n_{\mathbf{k}}$ in the crossover region $-1 \le 1/k_Fa \le 1$. Measurements of the momentum distribution of harmonically trapped systems have recently become available in the crossover [16]. The comparison carried out at unitarity, using the local density approximation, shows a good agreement with the observed distribution, but the experimental uncertainty is too large to distinguish between mean-field and FN DMC results [16].

The condensate fraction of pairs α has been obtained from the projected TBDM, defined as [17,18]

$$\rho_2^P(r) = \frac{2}{N}\int d^3\mathbf{r}_1 d^3\mathbf{r}_2 \rho_2(\mathbf{r}_1+\mathbf{r}, \mathbf{r}_2+\mathbf{r}, \mathbf{r}_1, \mathbf{r}_2). \quad (9)$$

By using Eq. (3) one finds that $\lim_{r\to\infty}\rho_2^P(r) = \alpha$. In terms of the order parameter, $F(|\mathbf{r}_1 - \mathbf{r}_2|) = \langle\psi_\uparrow(\mathbf{r}_1)\psi_\downarrow(\mathbf{r}_2)\rangle$, one has instead $\lim_{r\to\infty}\rho_2^P(r) = 2/n\int d^3\mathbf{r}'|F(r')|^2$. In Fig. 3 we show the results of $\rho_2^P(r)$. Effects due to the finite simulation box can be substantially reduced if one considers the decomposition: $\lim_{r\to\infty}\rho_2(\mathbf{r}_1+\mathbf{r}, \mathbf{r}_2+\mathbf{r}, \mathbf{r}_1, \mathbf{r}_2) = |F(|\mathbf{r}_1 - \mathbf{r}_2|)|^2 + \rho_1^2(r)$, accounting for the large r behavior of ρ_2 when $\rho_1(r)$ is small but not zero. From this result one finds for the asymptotic behavior of the projected TBDM: $\lim_{r\to\infty}\rho_2^P(r) = \alpha + (N/2)\times(2\rho_1(r)/n)^2$. In Fig. 3 we show results for the quantity $h(r) = \rho_2^P(r) - (N/2)(2\rho_1(r)/n)^2$, which smoothly converges to a constant for large distances. The results for the condensate fraction α, as obtained from the asymptotic behavior of $h(r)$, are shown in Fig. 4. In the BEC regime, the results reproduce the Bogoliubov quantum depletion of a gas of composite bosons $\alpha = 1 - 8\sqrt{n_m a_m^3}/3\sqrt{\pi}$, where $n_m = (n/2)$ is the density of molecules and $a_m = 0.6a$ is the dimer-dimer scattering length [10,19]. In the opposite

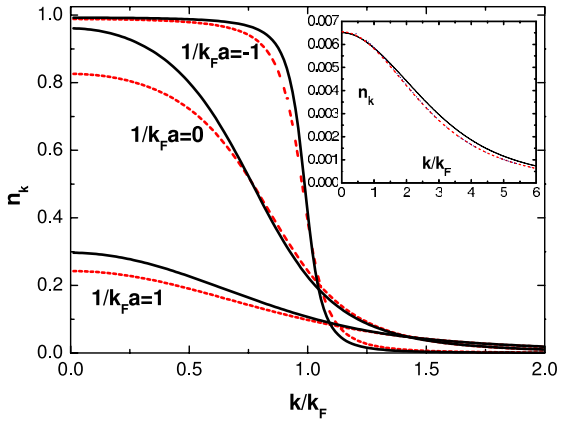

FIG. 2 (color online). Momentum distribution $n_{\mathbf{k}}$ for different values of $1/k_Fa$ (solid lines). The dashed lines (red online) correspond to $n_{\mathbf{k}}$ calculated using the BCS mean-field approach [15]. Inset: $n_{\mathbf{k}}$ for $1/k_Fa = 4$. The dotted line (blue online) corresponds to the momentum distribution of the molecular state $n_{\mathbf{k}} = 4(k_Fa)^3/[3\pi(1+k^2a^2)^2]$.

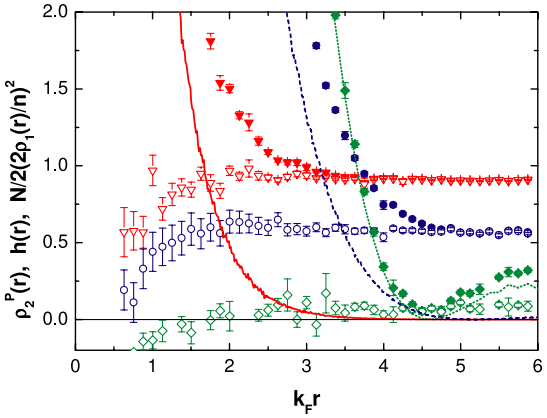

FIG. 3 (color online). Projected TBDM, $\rho_2^P(r)$, (solid symbols), $(N/2)[2\rho_1(r)/n)]^2$ (lines) and $h(r) = \rho_2^P(r) - (N/2)\times[2\rho_1(r)/n]^2$ (open symbols) for different values of $1/k_Fa$: $1/k_Fa = 1$ [solid line and triangles (red online)], $1/k_Fa = 0$ [dashed line and circles (blue online)] and $1/k_Fa = -1$ [dotted line and diamonds (green online)]. The condensate fraction of pairs α corresponds to the asymptotic behavior of $h(r)$.

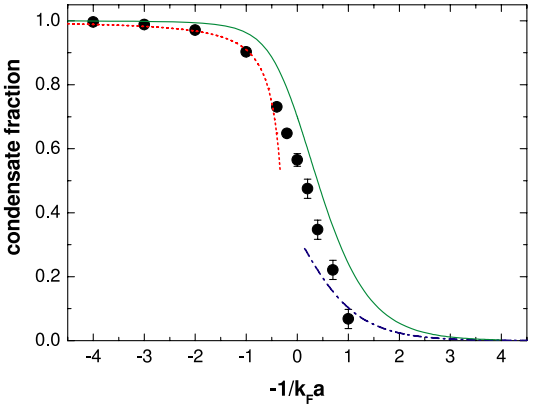

FIG. 4 (color online). Condensate fraction of pairs α as a function of the interaction strength: FN DMC results (symbols), Bogoliubov quantum depletion of a Bose gas with $a_m = 0.6a$ [dashed line (red online)], BCS theory using Eq. (10) [dot-dashed line (blue online)] and self-consistent mean-field theory [solid line (green online)].

BCS regime, the condensate fraction α can be calculated from the result of the BCS order parameter holding for $r \gg a$ [20]

$$F_{\mathrm{BCS}}(r) = \frac{\Delta k_F^3}{\epsilon_F} \frac{\sin(k_F r)}{4\pi^2 k_F r} K_0(r/\xi_0), \qquad (10)$$

where $\xi_0 = \hbar^2 k_F / m\Delta$ is the coherence length and $K_0(x)$ is the modified Bessel function. If we include the Gorkov–Melik-Barkhudarov correction for the pairing gap [21] $\Delta = (2/e)^{7/3} \epsilon_F e^{-\pi/2k_F|a|}$, we obtain for $\alpha = 2/n \int d^3\mathbf{r} F_{\mathrm{BCS}}^2(r)$ the dot-dashed line shown in Fig. 4. On the BEC side of the resonance, we notice that the agreement with the Bogoliubov quantum depletion, extending up to $1/k_F a \gtrsim 1$, is consistent with the evidence of the Lee-Huang-Yang beyond mean-field correction in the equation of state [10]. On the BCS side the comparison of the pairing gap Δ with the Gorkov–Melik-Barkhudarov result is discussed in Ref. [12]. We have checked that effects due to finite N are smaller than the statistical uncertainty. For example, at $1/k_F a = 0$, we find $\alpha = 0.57(2)$ for $N = 66$ and $\alpha = 0.61(2)$ for $N = 38$ particles. For $1/k_F a \leq -1$ the coherence length ξ_0 becomes increasingly larger and these effects start to be relevant. At $1/k_F a = -1$, the value of α, as obtained from $F_{\mathrm{BCS}}(r)$ [Eq. (10)], reduces from 0.10 to 0.08 by cutting off the spatial integral at the simulation box size $r = L/2$. The condensate fraction α can also be estimated using the self-consistent mean-field approach [9] and the result for the order parameter: $F(r) = (1/V)\sum_{\mathbf{k}} u_k v_k e^{i\mathbf{k}\cdot\mathbf{r}}$, where u_k and v_k are the usual quasiparticle amplitudes of BCS theory. The result is shown in Fig. 4 with a solid line (see also Ref. [18]).

In conclusion, we calculate using quantum Monte Carlo techniques the momentum distribution and the condensate fraction of pairs of a strongly interacting Fermi gas at zero temperature. Significant deviations from the mean-field description point out the role of correlations and quantum fluctuations in the BCS-BEC crossover.

G. E. A. and S. G. acknowledge support by the Ministero dell'Istruzione, dell'Università e della Ricerca (MIUR). J. B. and J. C. acknowledge support from DGI (Spain) Grant No. BFM2002-00466 and Generalitat de Catalunya Grant No. 2001SGR-00222.

[1] M. Greiner, C. A. Regal, and D. S. Jin, Nature (London) **426**, 537 (2003); S. Jochim *et al.*, Science **302**, 2101 (2003); M. W. Zwierlein *et al.*, Phys. Rev. Lett. **91**, 250401 (2003).
[2] M. Bartenstein *et al.*, Phys. Rev. Lett. **92**, 120401 (2004); T.Bourdel *et al.*, Phys. Rev. Lett. **93**, 050401 (2004).
[3] See, e.g., the recent review: Q. Chen, J. Stajic, S. Tan, and K. Levin, Phys. Rep. **412**, 1 (2005), and references therein.
[4] C. A. Regal, M. Greiner, and D. S. Jin, Phys. Rev. Lett. **92**, 040403 (2004); M. W. Zwierlein *et al.*, *ibid.* **92**, 120403 (2004).
[5] M. W. Zwierlein *et al.*, Phys. Rev. Lett. **94**, 180401 (2005).
[6] R. B. Diener and T.-L. Ho, cond-mat/0404517; A. Perali, P. Pieri, and G. C. Strinati, Phys. Rev. Lett. **95**, 010407 (2005); E. Altman and A. Vishwanath, Phys. Rev. Lett. **95**, 110404 (2005).
[7] C. N. Yang, Rev. Mod. Phys. **34**, 694 (1962).
[8] O. Penrose and L. Onsager, Phys. Rev. **104**, 576 (1956).
[9] A. J. Leggett, in *Modern Trends in the Theory of Condensed Matter*, edited by A. Pekalski and R. Przystawa (Springer-Verlag, Berlin, 1980); P. Nozières and S. Schmitt-Rink, J. Low Temp. Phys. **59**, 195 (1985); J. R. Engelbrecht, M. Randeria, and C. A. R. Sá de Melo, Phys. Rev. B **55**, 15 153 (1997).
[10] G. E. Astrakharchik, J. Boronat, J. Casulleras, and S. Giorgini, Phys. Rev. Lett. **93**, 200404 (2004).
[11] J. Carlson, S.-Y. Chang, V. R. Pandharipande, and K. E. Schmidt, Phys. Rev. Lett. **91**, 050401 (2003).
[12] S. Y. Chang, V. R. Pandharipande, J. Carlson, and K. E. Schmidt, Phys. Rev. A **70**, 043602 (2004).
[13] S. Y. Chang and V. R. Pandharipande, Phys. Rev. Lett. **95**, 080402 (2005).
[14] J. P. Bouchaud, A. Georges, and C. Lhuillier, J. Phys. (Paris) **49**, 553 (1988); J. P. Bouchaud and C. Lhuillier, Z. Phys. B **75**, 283 (1989).
[15] L. Viverit, S. Giorgini, L. P. Pitaevskii, and S. Stringari, Phys. Rev. A **69**, 013607 (2004).
[16] C. A. Regal *et al.*, cond-mat/0507316 (to be published).
[17] S. De Palo, F. Rapisarda, and G. Senatore, Phys. Rev. Lett. **88**, 206401 (2002).
[18] G. Ortiz and J. Dukelsky, Phys. Rev. A **72**, 043611 (2005); L. Salasnich, N. Manini, and A. Parola, Phys. Rev. A **72**, 023621 (2005).
[19] D. S. Petrov, C. Salomon, and G. V. Shlyapnikov, Phys. Rev. Lett. **93**, 090404 (2004).
[20] J. Bardeen, L. N. Cooper, and J. R. Schrieffer, Phys. Rev. **108**, 1175 (1957).
[21] L. P. Gorkov and T. K. Melik-Barkhudarov, Sov. Phys. JETP **13**, 1018 (1961).